High Relaxivity Gadolinium Hydroxypyridonate - Viral Capsid Conjugates: Nano-sized MRI Contrast Agents[1]

Ankona Datta[1], Jacob M. Hooker[1], Mauro Botta[2], Matthew B. Francis[1,3], Silvio Aime[4], and Kenneth N. Raymond[, 1]*

[1]Department of Chemistry, University of California, Berkeley, California 94720-1460; [2]Dipartimento di Scienze dell'Ambiente e della Vita, Universita` del Piemonte Orientale ''A. Avogadro'', Via Bellini 25/G, 15100 Alessandria, Italy; [3]Materials Sciences Division, Lawrence Berkeley National Labs, Berkeley, California 94720; [4]Dipartimento di Chimica IFM, Universita' di Torino, Via Giuria 7, 10125 Torino, Italy

AUTHOR EMAIL ADDRESS: raymond@socrates.berkeley.edu

ABSTRACT High relaxivity macromolecular contrast agents based on the conjugation of gadolinium chelates to the interior and exterior surfaces of MS2 viral capsids are assessed. The proton nuclear magnetic relaxation dispersion (NMRD) profiles of the conjugates show up to a five-fold increase in relaxivity, leading to a peak relaxivity (per Gd^{3+} ion) of 41.6 $mM^{-1}s^{-1}$ at 30 MHz for the internally modified capsids. Modification of the exterior was achieved through conjugation to flexible lysines, while internal modification was accomplished by conjugation to relatively rigid tyrosines. Higher relaxivities were obtained for the internally modified capsids, showing that (i) there is facile diffusion of water to the interior of capsids and (ii) the rigidity of the linker attaching the complex to the macromolecule is important for obtaining high relaxivity enhancements. The viral capsid conjugated gadolinium hydroxypyridonate complexes appear to possess two inner-sphere water molecules ($q = 2$) and the NMRD fittings highlight the differences in the local motion for the internal ($\tau_{Rl} = 440$ ps) and external ($\tau_{Rl} = 310$ ps) conjugates. These results indicate that there are significant advantages of using the internal surface of the capsids for contrast agent attachment, leaving the exterior surface available for the installation of tissue targeting groups.

MANUSCRIPT TEXT

Magnetic resonance imaging (MRI) is a routinely used noninvasive diagnostic technique, providing detailed images without the use of ionizing radiation. Although the resolution of MRI is excellent, its dynamic range is relatively narrow because of the limited variation in relaxation rates exhibited by water protons *in vivo*. When these differences are insufficient to distinguish between adjacent tissues, contrast enhancement is often achieved through the administration of synthetic agents that increase the water proton relaxation rates in accessible locations. Gadolinium complexes are the most often used for this purpose, with more than 10 million MRI studies being performed through their use each year.[2-4] The current commercially available Gd(III)-based contrast agents use poly(amino-carboxylate) chelates, and typically gram quantities of Gd must be injected to reach concentrations sufficient for usable contrast enhancement. However, this strategy is more difficult to apply to the specific imaging of biomarkers present in low (μM - nM) concentrations. To distinguish these sites from the background signal, targetable contrast agents will undoubtedly require significantly improved contrast enhancement efficiencies.[3, 5]

MRI contrast agents are commonly evaluated on the basis of relaxivity (r_{1p}), which describes their ability to increase the longitudinal relaxation rate of nearby water molecule protons per millimolar concentration of agent applied.[6] Strategies for enhancing the relaxivity of contrast agents include increasing the number of bound water molecules (q), optimizing the water-residence time (τ_M) and increasing the rotational correlation time (τ_R) by attachment to macromolecules or nanoparticles. The first two parameters have been optimized successfully in Gd hydroxypyridonate (HOPO) based contrast agents, and when attached to macromolecules relaxivities as high as 200 mM^{-1}s^{-1} per Gd (peaking between 20-100 MHz, with $q = 2$, $r_{Gd-H} = 3.1$ and electronic relaxation times T$_{1e}$ = 15 ns, T$_{2e}$= 0.3 ns) can theoretically be obtained for these complexes.[7] For HOPO based and other complexes, relaxivity enhancement has been demonstrated through the attachment of contrast agents to proteins,[8-10] polypeptides,[11] dendrimers,[12, 13] nanospheres,[14] and micellar nanoparticles.[15-17] Nanometer scale contrast agents also offer the potential to differentiate non-nervous-system tissue. They should be large enough to be retained in blood capillaries by normal endothelial barriers, and yet they should diffuse across the distorted endothelium associated with pathological lesions.[9, 11] Studies have shown that particles larger than 10 nm should be able to permeate preferentially through tumor tissues.[11]

Recently, several groups have explored the idea of using the protein coats of viruses as potential nanoparticles for the development of nanometer scale MRI contrast agents. The availability of two surfaces (inside and outside) can allow the independent attachment of imaging and targeting agents to the same scaffold, providing an advantage over most common approaches to macromolecular contrast agents. The first demonstration of this concept involved the chelation of Gd^{3+} ions to Ca^{2+} binding sites in the protein coat of the cowpea chlorotic mottle virus (CCMV, 28.5 nm diameter). The resulting particles exhibited exceedingly high relaxivities (r_{1p} = 202 mM^{-1}s^{-1} per Gd ion at 61 MHz),[18] but clinical applications will require improvements in metal binding affinity to avoid the toxicity of free gadolinium. Another study involved the conjugation of Magnevist (Gd-diethylenetriaminopentaacetic acid, Gd-DTPA) isothiocyanate to lysine residues of MS2 virus capsids.[19] The resulting relaxivity was 14 mM^{-1}s^{-1} per Gd ion, with a total molecular relaxivity of 7200 mM^{-1}s^{-1} at 64 MHz. 'Click chemistry' has also been used for the covalent attachment of Gd(DOTA) to lysine residues, in conjunction with the natural affinity of Gd^{3+} ions for the polynucleotide encapsulated within the capsids. These conjugates exhibited similar relaxivities (11-15 mM^{-1}s^{-1} per complex at 64 MHz).[20]

These examples demonstrate that viral capsids offer significant potential for building nanometer scale contrast agents with very high overall relaxivities. They also indicate that a balance must be struck between the high relaxivity of weakly bound Gd^{3+} and the need for strong chelators that reduce toxicity at the expense of available water exchange sites. Several factors related to the linking strategy (such as the rigidity of the linkers, the interaction of Gd-complexing ligands with protein residues, and the flexibility of the protein region containing the amino acid being modified) may also affect the overall relaxivity values in complex ways.[21-24] Therefore, detailed studies of the relaxometric properties are needed to determine the influence of these factors.

To do this, we report herein a detailed analysis of the NMRD profiles and physical parameters of two viral-capsid based contrast agents. Recently we have described the covalent attachment of HOPO based chelates to either the exterior or the interior surface of bacteriophage MS2 capsids devoid of nucleic acids.[25] The MS2 capsid shell consists of 180 copies of the coat protein (MW = 13.7 kDa) assembled into an icosahedral arrangement (diameter 27 nm). A Gd^{3+} ligand suitably functionalized for selective bioconjugation (**1**) was prepared by attaching an alkoxyamine linker to a heteropodal TREN-bis-HOPO-TAM ligand.[26] This compound was then attached to capsids previously modified by attaching aldehyde groups to exterior amino groups (K106, K113, and the *N*-terminus, 540 total sites per capsid) or interior tyrosines (Y85, 180 total sites per capsid),[27] Figure 1. Due to the lower solubility of the external conjugates, the number of ligands per capsid was chosen to be 90 (50% functionalization). The resultant conjugates were then metallated with Gd^{3+} to obtain the contrast agents shown in Figure 2.[28] Free Gd^{3+} was removed through exhaustive dialysis against citrate buffer, as has been previously described.[25]

The Gd-HOPO chelates were chosen because they have at least 2-3 times higher relaxivities (between 8-14 mM^{-1}s^{-1} at 20 MHz) than those of commercial agents, while maintaining similar stabilities (TREN-bis-HOPO-TAM-Me, pGd 20.1; Gd-DTPA, pGd 19.4).[29-31] The higher relaxivities of the HOPO-based complexes are primarily due to an increased number of bound water molecules ($q = 2$ or 3) and fast water exchange (τ_M typically between 5 and 30 ns[32-34]). These values represent exchange rates that are orders of magnitude faster than those of commercial complexes and are near optimal for attaining maximum relaxivities for molecules having very slow tumbling rates (e.g. oligomers and contrast agents attached to dendrimers). The initial relaxivity measurements on the Gd-HOPO-capsid conjugates gave relaxivities per Gd^{3+} ion as high as 41.6 mM^{-1}s^{-1} (at 30 MHz and 25 ºC), values that represent some of the highest relaxivities yet reported for covalently modified virus-based contrast agents.

Anticipating the biological relevance of these studies, full relaxometric data have been obtained at both 310 and 298 K. The change of relaxivity with magnetic field is a NMRD profile that can be fitted to the appropriate model describing the magnetic coupling of the solvent with the system. Important parameters, such as q, τ_M, and τ_R that affect relaxivity can then be obtained from the fits. The NMRD profiles for the externally and internally modified HOPO-capsid conjugates compared to that of small molecule chelate Gd-TREN-bis-HOPO-TAM-CO$_2$H are shown in Figures 3 and 4.[30] The maximum relaxivities obtained were 30.7 mM^{-1}s^{-1} (30 MHz, 25 ºC) for the externally modified capsids and 41.6 mM^{-1}s^{-1} (30 MHz, 25 ºC) for the internally modified capsids. This represents a four to five fold increase in relaxivity upon attachment of the Gd-TREN-bis-HOPO-TAM chelate to virus capsids in comparison to Gd-TREN-bis-HOPO-TAM-CO$_2$H. The relaxation rate of unlabeled MS2 was measured to be ca. 0.4-0.5 s^{-1} and showed a negligible dependence on the magnetic field strength. The relaxivity values decrease (27.8 mM^{-1}s^{-1} for external and 38.9 mM^{-1}s^{-1} for internal modification, at 30 MHz) upon increasing the temperature to 37 ºC, suggesting that the relaxivity enhancements observed upon conjugation to the MS2 capsids are not limited by a slow rate of water exchange from the inner coordination sphere of Gd(III), but rather by the tumbling rate. The temperature dependence of relaxivity (r_{1p}, longitudinal relaxivity) for the externally and internally modified capsids at 20 MHz is shown in Figure 5. The exponential decrease of relaxivity with increasing temperature is consistent with slowly tumbling systems with fast-exchanging inner-sphere water molecules.

Solomon-Bloembergen-Morgan theory connects the macroscopic relaxivity to the intrinsic parameters of the Gd(III) complexes.[6, 35] High frequency data (2-70 MHz) were fitted to this relationship for paramagnetic relaxation, modified in terms of the Lipari-Szabo approach for the description of the rotational dynamics.[36-38] This model considers two types of motion that influence the magnetic relaxation: global motion of the system described by a global reorientation correlation time τ_{Rg}, and faster local motion with a local reorientation correlation time τ_{Rl}. An additional parameter, S^2, describes the extent of spatial restriction of the local motion (or the coupling of local and global motions); $S^2 = 1$ when the Gd-complex is completely immobilized ($\tau_{Rg} = \tau_{Rl}$), and $S^2 = 0$ when the local motion is totally independent of the global motion of the system. The parameters for electronic relaxation (Δ^2, τ_V) were used as empirical fitting parameters and do not have a precise physical meaning in this model. For this reason, these parameters were not forced to be identical for the internal and external conjugates. The outer-sphere component of the relaxivity was estimated on the basis of the Freed equation by using standard values for the distance of closest approach a and the relative diffusion coefficient of solute and solvent D.[6]

The parameters that gave the best fit for the NMRD profiles are listed in Table 1. The number of inner sphere molecules (q) has been reported as 2 for the TREN-bis-HOPO-TAM complexes. The q value is reliably estimated by analysis of the NMRD profiles and by comparison of the relaxivity data for a large series of related complexes.[30] The validity of the relaxometric evaluation of the hydration number has been confirmed through the direct measurement of q by luminescence in the case of EuTACN-1,2-HOPO ($q = 3$)[33] and Eu-H(2,2)-1,2-HOPO ($q = 1$).[39] The NMRD profile fits for the

conjugates were obtained by fixing q to 2. Although the hypothesis that both conjugated complexes possess $q=1$ cannot be excluded on the basis of the relaxometric data, the assumption of two bound water molecules gave the best fits (Supporting information Figure S1) for both the internally and externally modified capsids, and is consistent with other TREN-bis-HOPO-TAM derivatives.[7, 30] The distance of the coordinated water molecules from the metal ion (r_{Gd-H}) was fixed to 3.1 Å.[40] Based on the observed relaxivity dependence with temperature and on the analogy with other Gd-TREN-bis-HOPO-TAM derivatives, the mean residence lifetime τ_M was fixed to 10 ns (Supporting information Figures S2 and S3).[30] Facile diffusion of water to the interior of the capsid is implied by the result that the best NMRD fits for **4** and **5** (internal conjugates **5** with slightly higher relaxivity values, compared to external conjugates **4**) were for the same q value for both conjugates. The internal conjugates also have greater solubility than the external conjugates, and hence present the advantage of attaching solubilizing and targeting groups to the exterior.[25]

The τ_R value for Gd-TREN-bis-HOPO-TAM-CO$_2$H has been reported as 94 ps at 298 K (Table 2).[30] The local reorientation correlation times (τ_{Rl}) can be compared to the τ_R value for the small molecule complex and is 3 to 4 times slower for the conjugates (310 ps for the external and 440 ps for the internal conjugates). Also, the value for the internal conjugates is 1.4 times slower than the external conjugates. The external conjugates were obtained by covalent linkages to lysines, while the internal conjugates were obtained by forming covalent linkages to tyrosines. Targeting a rigid aromatic tyrosine residue side chain, rather than a more flexible aliphatic lysine side chain, reduces the number of free rotating σ-bonds between the Gd-chelate and the capsid surface. The increased rigidity of the tyrosine-based bioconjugation strategy could be responsible for the slower τ_{Rl}. In addition, we must consider that the amount of protein structural fluctuation is different at the sites of attachment (Y85 versus the amino groups). The MS2 capsid shell is dynamic in solution, and motion about or around loop regions may affect τ_{Rl}. The lysines are a part of α-helices and the tyrosines are a part of β-sheets, as shown in Figure 6, and the difference in the rigidities of these local protein environments can affect the τ_{Rl} values (β-sheets being more rigid than α-helices). Thus, the τ_{Rl} values reflect relatively accurately the local rigidity of the conjugates and hence the difference in relaxivities for the internal and external conjugates (the maximum relaxivity for the internal conjugates was 1.35 times higher than the external conjugates).

The global reorientation correlation times, τ_{Rg}, should be very similar for the two conjugates as well as close to the rotational correlation time value of the MS2 virus capsid. This value has been reported to be close to 1 μs.[41] The results of the NMRD fits were not sensitive to the τ_{Rg} value in the range of 100 ns – 1 ms, so this value was set to 1 μs. The parameter S^2, which indicates the effect of the global reorientation on local reorientation motion, or the coupling of the two motions, also has a low value in the range of 0.08-0.14. The values are again slightly higher for the internal conjugates, indicating greater coupling between the local and global motions.

The parameters obtained for these Gd-HOPO virus conjugates can be compared to the parameters reported for Gd-DOTA (commercially available as DOTAREM)[42] dendrimer based conjugates, Gadomer 17[21] and PAMAM-G4-[Gd(DOTA-pBn)(H$_2$O)]$^-_{33}$[43] (Table 2). These dendrimeric conjugates are obtained through the covalent attachment of multiple Gd-DOTA units to polyamine based dendrimers. Their NMRD profiles have been analyzed according to the Lipari-Szabo approach.[21, 43] Gd-DOTA has a longer water-residence time ($\tau_M = 244$ ns)[42] than Gd-HOPO-based contrast agents ($\tau_M = 10$ ns), which inherently limits the relaxivity enhancements that can be attained upon conjugation to macromolecules. The τ_{Rl} and S^2 values for both of the dendrimer based conjugates are higher than those obtained for our virus based conjugates (indicating that these dendrimer based systems are more rigid that the capsid based systems), and the relaxivity enhancements (upon attachment to dendrimers) are in the range of 3.5 to 6.5 times those of the Gd-DOTA monomer (at 20 MHz and 25 °C). These relaxivity enhancements are similar to the values obtained for the virus-based conjugates (3.7 times for conjugate **4** and 5.3 times for conjugate **5** at 20 MHz relative to the Gd-HOPO monomer); however this cannot be completely explained by the τ_{Rl} and S^2 values, which are lower for virus based systems. For

4

example, conjugate **4** has τ_{Rl} = 310 ps and S^2 = 0.08, while Gadomer 17 has τ_{Rl} = 760 ps and S^2 = 0.5, even though slightly greater relaxivity enhancements are observed for conjugate **4**.

Improved relaxivities are obtained in the Gd-DOTA based systems when the water exchange becomes faster, as in PAMAM-G4-[Gd(DOTA-pBn)(H$_2$O)]$^-$33, due to the presence of a *p*Bn substituent on the Gd-DOTA that decreases the water residence time due to conformational or steric effects.[43] The major difference in these systems is the mean water-residence lifetime (τ_M = 152 ns and 1000 ns for the Gd-DOTA dendrimer conjugates, while τ_M < ca. 50 ns for the Gd-HOPO virus conjugates). In the case of the Gd-DOTA based systems, the substitution position on the Gd-DOTA complex to create the attachment point to dendrimers affects the water residence time.[21, 43] For Gd-TREN-bis-HOPO-TAM based systems, substituents on the TAM ligands lead to the water residence time in the range of 2-20 ns[30], and hence as mentioned previously τ_M = 10 ns was chosen for the virus conjugates to obtain the best fits for the NMRD profiles. The reason for the relaxivity enhancements observed can then be attributed to the optimal water exchange rates (in addition to the slow rotational correlation times) for the Gd-HOPO based systems, which would also lead to improved relaxivities for these macromolecular contrast agents at higher field strengths when compared to Gd-DOTA based system.[7, 42]

The NMRD profiles and the temperature dependence studies of these capsid systems indicate that they can be further improved to provide systems with sufficiently high relaxivity for biomarker targeting. Theoretical predictions for these systems (Figure **7**) indicate that upon increasing the local reorientation correlation through the use of more rigid linkers, the relaxivity values can be increased to 140 mM^{-1}s^{-1} per Gd^{3+} ion at clinically relevant fields. Linking through tyrosine residues may be inherently beneficial in this respect, since they have fewer rotatable bonds than lysines. The observation that water transport through the capsid shell is not rate limiting suggests that additional complexes can be installed to reach still higher total relaxivity, a concept that is enabled by the increased water solubility of the internally modified conjugates. According to the theoretical predictions (Figure **7**) and our data at 60 MHz (Table 2), the relaxivity increase upon increasing the rigidity will be limited as we move to higher field strengths, for targeted imaging applications. Higher relaxivities can be attained in these cases by using Gd chelates with smaller τ_M values (1-2 ns) optimal for higher field strengths, in conjunction to rigid linkers. The use of the Gd-TACN-HOPO-based complexes with such optimal water-exchange rates and a higher number of inner sphere water molecules (q=3) [33] should enhance the obtained relaxivities, as predicted in this study. The generation of additional capsid conjugates that possess these properties is currently in progress in our laboratories.

Experimental Section

Field cycling relaxometry The water proton NMRD profiles were measured at 25 and 37 °C on a Stelar Fast Field-Cycling Spectrometer FFC–2000 (Mede, Pv, Italy) on about 0.2-0.4 mmol complex-conjugated MS2 solutions in non-deuterated water. The ^{1}H T_1 relaxation times were acquired by the standard inversion recovery method with a typical 90° pulse width of 3.5 µs, using 16 experiments of 4 scans. The reproducibility of the T_1 data was ±4%. The temperature was controlled with a Stelar VTC-91 airflow heater equipped with a calibrated copper–constantan thermocouple (uncertainty of ± 0.1 °C). The NMRD profiles were measured in the range of magnetic fields from 0.00024 to 1.6 T (corresponding to 0.01–70 MHz proton Larmor frequencies).

Gd-content measurements: Mineralization Monitored by Relaxometry[44]
The gadolinium concentration of the complex-conjugated MS2 solutions was measured by a relaxometric procedure (20 MHz and 25 °C). Three accurate determinations (each on 3 different samples of similar concentration, prepared by dilution) of the ^{1}H longitudinal water proton relaxation rate (R$_1$^{obs}) were made at pH=6.9 on ca. 0.2-0.5 mM aqueous solutions. A volume of 100 µL of each solution was then added to 100 µL of 70 % HNO$_3$ directly into a 1.0 mL glass ampoule. After gentle centrifugation (to ensure complete mixing) of the resulting solutions (1500 rpm, 2 min) the ampoules

were sealed and heated at 120 °C for 5 days. This treatment ensures that all Gd(III) is solubilized. The R_1 values (R_1^*) were then measured again (three times) and the concentration of Gd(III) in the starting solutions calculated using the following expression:

$$[Gd] = [(R_1^* - 0.51)/13.99] \times 2 \qquad (1)$$

where 13.99 is the relaxivity ($mM^{-1} s^{-1}$) of the Gd ion under identical experimental conditions and 0.51 (s^{-1}) the relaxation rate of the diamagnetic solution (1:1 water and HNO_3 70 %). This procedure was validated either on two solutions of know concentration (GdDTPA and GdDOTA) or by comparing the relaxometric procedure with the ICP data (on GdDTPA).

Variable temperature measurements The temperature dependence of the longitudinal water proton relaxation rates was measured on a Stelar Spin-Master spectrometer operating at a magnetic field strength of 0.47 T (corresponding to the proton Larmor frequency of 20 MHz). The standard inversion–recovery pulse sequence (180° –τ –90°) was used. The samples (ca. 100 μL) were placed in 5 mm NMR tubes. The temperature was controlled by a Stelar VTC-91 air flow heater equipped with a copper–constantan thermocouple. The desired temperature was set up either by the internal heater or by an attached liquid nitrogen evaporator (T<24 °C). The actual temperature was checked inside the probehead (uncertainty of ± 0.1 °C) by using a digital thermometer.
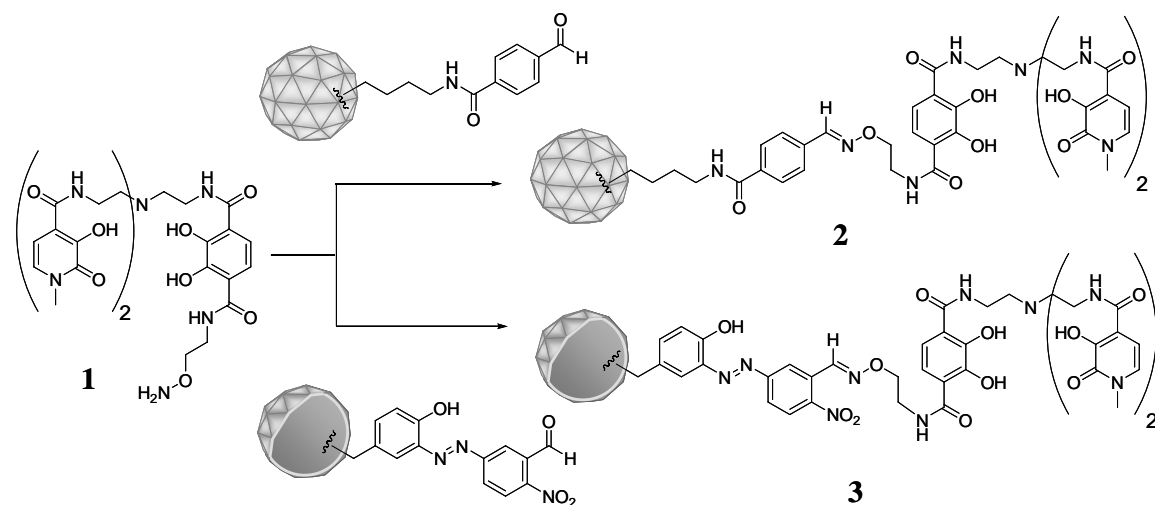
FIGURES

Figure 1. Conjugation of the TREN-bis-HOPO-TAM ligand to the exterior (**2**, targeting K106, K113, and the *N*-terminus) and interior (**3**, targeting Y85) surfaces of empty MS2 capsids. The conjugation was controlled to give 90 ligands per capsid in both cases.
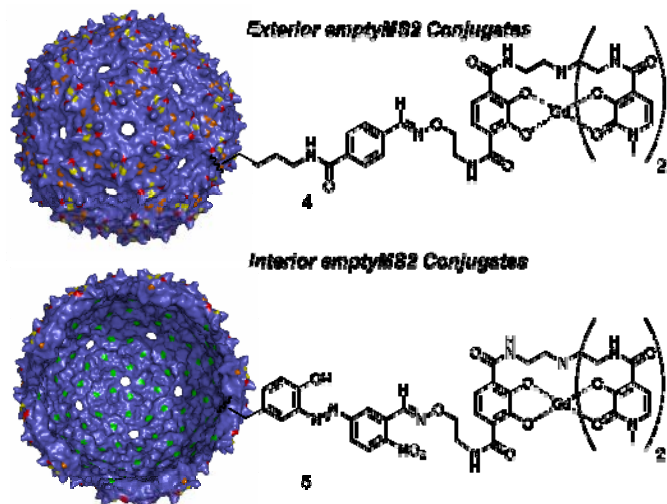
Figure 2. Externally (**4**) and internally (**5**) labeled macromolecular contrast agents obtained upon metallation of the capsid conjugates with gadolinium(III). The crystal structure of the MS2 virus capsid is shown,[28] highlighting the amino groups on the exterior: red = K106, yellow = K113, and orange = the *N*-terminus. Y85 is highlighted in green on the interior surface.
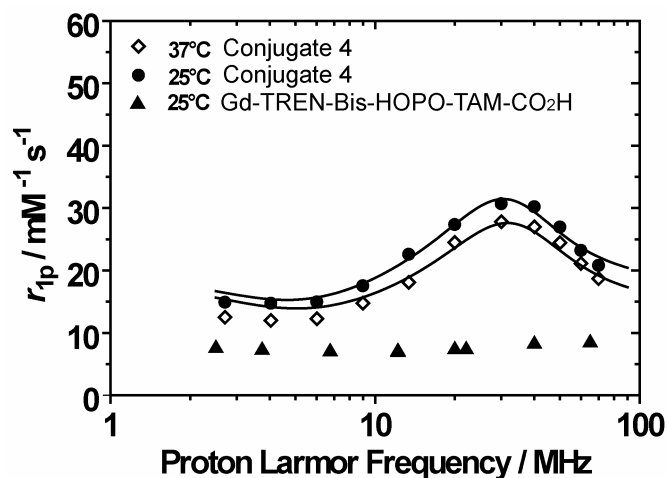

Figure 3. $1/T_1$ proton nuclear magnetic relaxation dispersion (NMRD) profiles (pH = 6.9) and fits for conjugate **4** at 25 ºC (filled circles) and 37 ºC (open diamonds), in comparison with the NMRD profile for Gd-TREN-bis-HOPO-TAM-CO$_2$H at 25 ºC (filled triangles).[30]
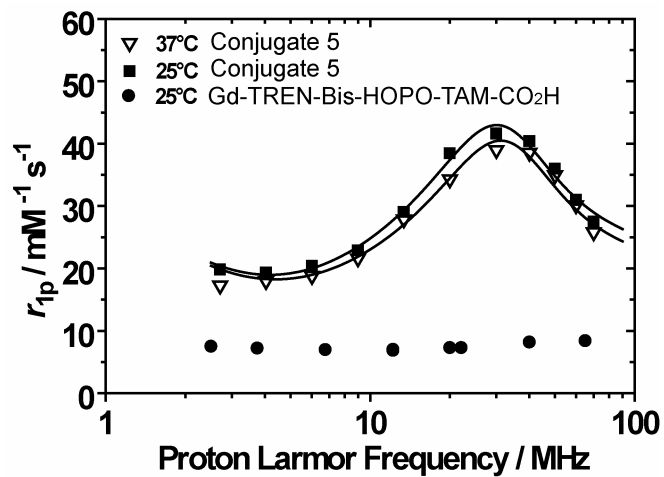
Figure 4. $1/T_1$ proton nuclear magnetic relaxation dispersion (NMRD) profiles (pH = 6.9) and fits for conjugate **5** at 25 (filled squares) and 37 ºC (open triangles), in comparison with the NMRD profile for Gd-TREN-bis-HOPO-TAM-CO$_2$H at 25 ºC (filled circles).[30]
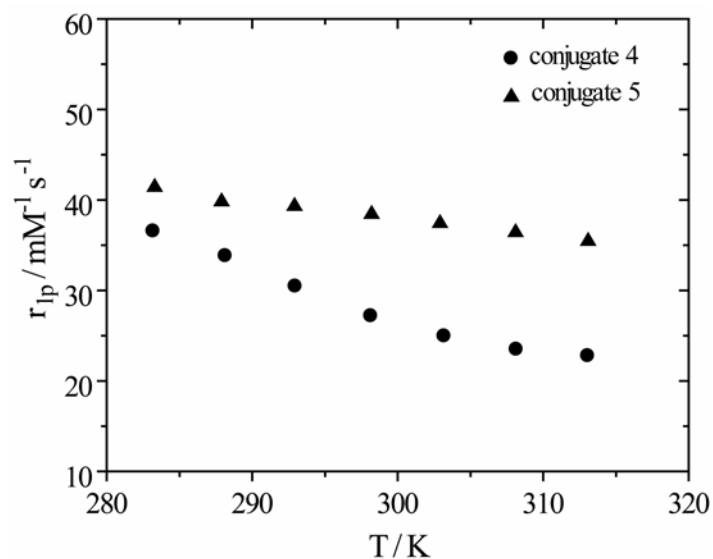

Figure 5. Variable-temperature proton relaxivity for conjugates **4** (filled circles) and **5** (filled triangles) at 20 MHz.
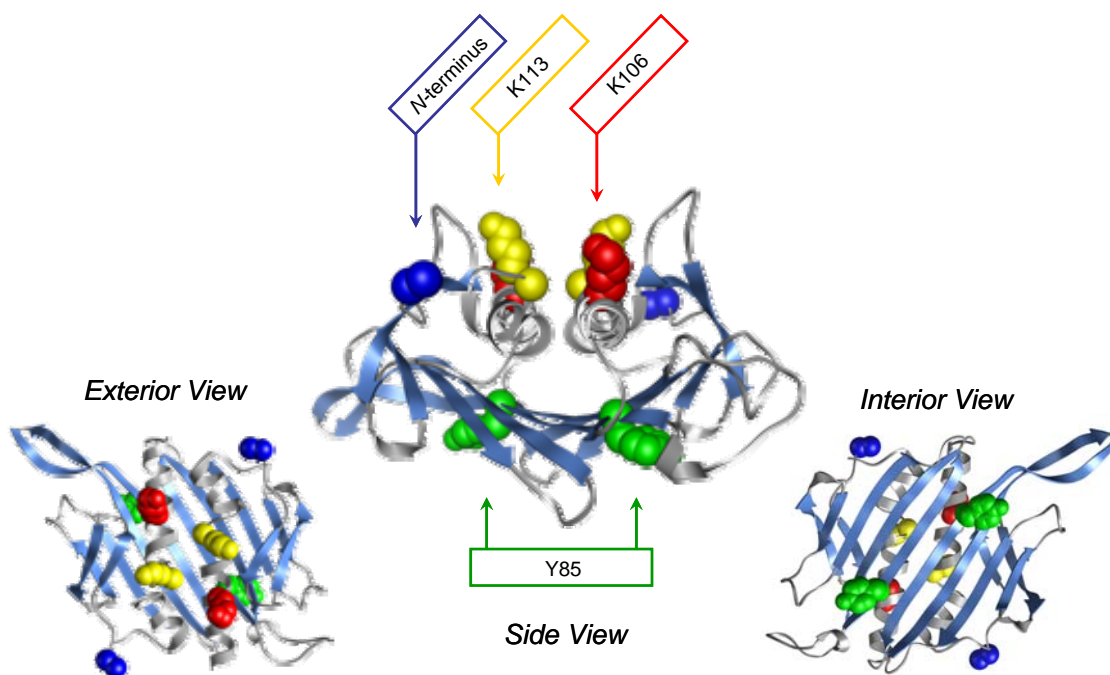
Figure 6. The locations of the modified protein residues shown in the exterior, side, and interior views, as mapped on a coat protein dimer. Y85 extends from a β-sheet in the interior, while K106 and K113 extend from α-helices on the exterior, causing differences in the local environments of the amino acids being modified.
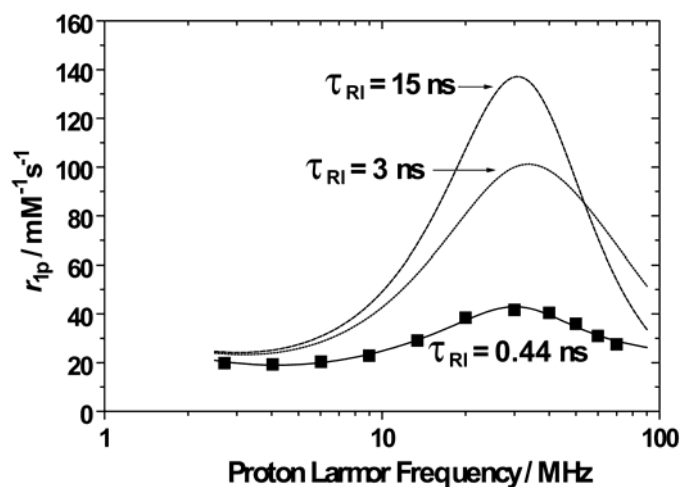

Figure 7. Theoretical predictions for the maximum relaxivity attainable if the linkages are further rigidified to restrict the local motion (modeled using the parameters obtained for the internal conjugates at 298 K).

9

TABLES.

Table 1. Fitting parameters for the NMRD profiles of the macromolecular complexes **4** and **5**.

	4^a (exterior)		**5^a (interior)**	
	298 K	310 K	298 K	310 K
r_{1p} (mM^{-1}s^{-1})^b	30.7	27.8	41.6	38.9
Δ^2 (10^{19} s^{-2})	2.4 ± 0.3	2.5 ± 0.4	1.6 ± 0.2	1.7 ± 0.1
τ_V (ps)	36 ± 2	34 ± 1	24 ± 2	21 ± 3
τ_{Rl} (ns)	0.31 ± 0.01	0.25 ± 0.01	0.44 ± 0.02	0.40 ± 0.01
τ_{Rg} (μs)^c	1	1	1	1
τ_M (ns)^c	10	10	10	10
S^2	0.08 ± 0.01	0.09 ± 0.01	0.13 ± 0.01	0.14 ± 0.01
q^c	2	2	2	2
r_{Gd-H} (Å)^c	3.1	3.1	3.1	3.1
a (Å)^c	4.0	4.0	4.0	4.0
D (10^5 cm^{2}s^{-1})^c	2.3	3.1	2.3	3.1

^{a} determined in 12.5 mM HEPES buffer at pH 6.85. ^{b} relaxivity data at 30 MHz. ^{c} Parameter fixed prior to fitting.

Table 2. Comparison of the parameters (at 25 °C) obtained for conjugates **4** and **5** with dendrimer based macromolecular contrast agents.

Complex	τ_M (ns)	τ_{Rg} (ns)	τ_{Rl} (ps)	S^2	r_{1p}(20 MHz) (mM^{-1}s^{-1})	r_{1p}(60 MHz) (mM^{-1}s^{-1})	Reference
Gd-TREN-bis-HOPO-TAM-CO$_2$H	10	-	94	-	7.3	8.5	30
Gd-DOTA	244	-	77	-	4.74	3.7	42
Gadomer 17	1000	3.05	760	0.5	16.5	16.4	21
PAMAM-G4-[Gd(DOTA-pBn)(H$_2$O)]$^-_{33}$	152	3.10	550	0.39	31.2	22.5	43
External conjugate **4**	10	1000	310	0.08	27.3	23.2	This work
Internal conjugate **5**	10	1000	440	0.13	38.4	30.9	This work

REFERENCES

(1) High Relaxivity Gadolinium MRI Agents. 23. Part 22: Jocher, C. J.; Moore, E. G.; Xu, J.; Avedano, S.; Botta, M.; Aime, S.; Raymond, K. N., *Inorg. Chem.* **2007,** 46, (22), 9182-9191.
(2) Bottrill, M.; Nicholas, L. K.; Long, N. J., *Chem. Soc. Rev.* **2006,** 35, (6), 557-571.
(3) Caravan, P., *Chem. Soc. Rev.* **2006,** 35, (6), 512-523.
(4) Lowe, M. P., *Aust. J. Chem.* **2002,** 55, (9), 551-556.
(5) Jaffer, F. A.; Weissleder, R., *JAMA-J. Am. Med. Assoc.* **2005,** 293, (7), 855-862.
(6) Aime, S.; Botta, M.; Terreno, E., *Gd(III)-based Contrast Agents for MRI*. Elsevier: San Diego, 2005; Vol. 57, p 173-237.
(7) Raymond, K. N.; Pierre, V. C., *Bioconjugate Chem.* **2005,** 16, (1), 3-8.
(8) Aime, S.; Botta, M.; Fasano, M.; Terreno, E., *Chem. Soc. Rev.* **1998,** 27, (1), 19-29.
(9) Barrett, T.; Kobayashi, H.; Brechbiel, M.; Choyke, P. L., *Eur. J. Rad.* **2006,** 60, (3), 353-366.
(10) Muller, R. N.; Raduchel, B.; Laurent, S.; Platzek, J.; Pierart, C.; Mareski, P.; Vander Elst, L., *Eur. J. Inorg. Chem.* **1999**, (11), 1949-1955.
(11) Daldrup-Link, H. E.; Brasch, R. C., *Eur. Radiol.* **2003,** 13, (2), 354-365.
(12) Pierre, V. C.; Botta, M.; Raymond, K. N., *J. Am. Chem. Soc.* **2005,** 127, (2), 504-505.
(13) Rudovsky, J.; Botta, M.; Hermann, P.; Hardcastle, K. I.; Lukes, I.; Aime, S., *Bioconjugate Chem.* **2006,** 17, (4), 975-987.
(14) Turner, J. L.; Pan, D. P. J.; Plummer, R.; Chen, Z. Y.; Whittaker, A. K.; Wooley, K. L., *Adv. Funct. Mater.* **2005,** 15, (8), 1248-1254.
(15) Accardo, A.; Tesauro, D.; Morelli, G.; Gianolio, E.; Aime, S.; Vaccaro, M.; Mangiapia, G.; Paduano, L.; Schillen, K., *J. Biol. Inorg. Chem.* **2007,** 12, (2), 267-276.
(16) Briley-Saebo, K. C.; Amirbekian, V.; Mani, V.; Aguinaldo, J. G. S.; Vucic, E.; Carpenter, D.; Amirbekian, S.; Fayad, Z. A., *Magn. Reson. Med.* **2006,** 56, (6), 1336-1346.
(17) Nicolle, G. M.; Toth, E.; Eisenwiener, K. P.; Macke, H. R.; Merbach, A. E., *J. Biol. Inorg. Chem.* **2002,** 7, (7-8), 757-769.
(18) Allen, M.; Bulte, J. W. M.; Liepold, L.; Basu, G.; Zywicke, H. A.; Frank, J. A.; Young, M.; Douglas, T., *Magn. Reson. Med.* **2005,** 54, (4), 807-812.
(19) Anderson, E. A.; Isaacman, S.; Peabody, D. S.; Wang, E. Y.; Canary, J. W.; Kirshenbaum, K., *Nano Lett.* **2006,** 6, (6), 1160-1164.
(20) Prasuhn, D. E.; Yeh, R. M.; Obenaus, A.; Manchester, M.; Finn, M. G., *Chem. Comm.* **2007**, (12), 1269-1271.
(21) Nicolle, G. M.; Toth, E.; Schmitt-Willich, H.; Raduchel, B.; Merbach, A. E., *Chem.-Eur. J.* **2002,** 8, (5), 1040-1048.
(22) Zech, S. G.; Eldredge, H. B.; Lowe, M. P.; Caravan, P., *Inorg. Chem.* **2007,** 46, (9), 3576-3584.
(23) Aime, S.; Frullano, L.; Crich, S. G., *Angew. Chem., Int. Ed. Engl.* **2002,** 41, (6), 1017-1019.
(24) Vasalatiy, O.; Zhao, P.; Zhang, S.; Aime, S.; Sherry, A. D., *Contrast Media Mol Imaging* **2006,** 1, (1), 10-14.
(25) Hooker, J. M.; Datta, A.; Botta, M.; Raymond, K. N.; Francis, M. B., *Nano Lett.* **2007,** 7, (8), 2207-2210.
(26) Cohen, S. M.; Xu, J. D.; Radkov, E.; Raymond, K. N.; Botta, M.; Barge, A.; Aime, S., *Inorg. Chem.* **2000,** 39, (25), 5747-5756.
(27) Hooker, J. M.; Kovacs, E. W.; Francis, M. B., *J. Am. Chem. Soc.* **2004,** 126, (12), 3718-3719.
(28) Valegard, K.; Liljas, L.; Fridborg, K.; Unge, T., *Nature* **1990,** 345, (6270), 36-41.
(29) Doble, D. M. J.; Melchior, M.; O'Sullivan, B.; Siering, C.; Xu, J. D.; Pierre, V. C.; Raymond, K. N., *Inorg. Chem.* **2003,** 42, (16), 4930-4937.
(30) Pierre, V. C.; Botta, M.; Aime, S.; Raymond, K. N., *Inorg. Chem.* **2006,** 45, (20), 8355-8364.
(31) Pierre, V. C.; Melchior, M.; Doble, D. M. J.; Raymond, K. N., *Inorg. Chem.* **2004,** 43, (26), 8520-8525.

(32) Thompson, M. K.; Botta, M.; Nicolle, G.; Helm, L.; Aime, S.; Merbach, A. E.; Raymond, K. N., *J. Am. Chem. Soc.* **2003,** 125, (47), 14274-14275.

(33) Werner, E. J.; Avedano, S.; Botta, M.; Hay, B. P.; Moore, E. G.; Aime, S.; Raymond, K. N., *J. Am. Chem. Soc.* **2007,** 129, (7), 1870-1871.

(34) Xu, J.; Franklin, S. J.; Whisenhunt, D. W.; Raymond, K. N., *J. Am. Chem. Soc.* **1995,** 117, (27), 7245-7246.

(35) Caravan, P.; Ellison, J. J.; McMurry, T. J.; Lauffer, R. B., *Chem. Rev.* **1999,** 99, (9), 2293-2352.

(36) Lipari, G.; Szabo, A., *J. Am. Chem. Soc.* **1982,** 104, (17), 4546-4559.

(37) Lipari, G.; Szabo, A., *J. Am. Chem. Soc.* **1982,** 104, (17), 4559-4570.

(38) Zhang, Z. D.; Greenfield, M. T.; Spiller, M.; McMurry, T. J.; Lauffer, R. B.; Caravan, P., *Angew. Chem., Int. Ed. Engl.* **2005,** 44, (41), 6766-6769.

(39) Jocher, C. J.; Botta, M.; Avedano, S.; Moore, E. G.; Xu, J.; Aime, S.; Raymond, K. N., *Inorg. Chem.* **2007,** 46, (12), 4796-4798.

(40) Caravan, P.; Astashkin, A. V.; Raitsimring, A. M., *Inorg. Chem.* **2003,** 42, (13), 3972-3974.

(41) Kang, J. S.; Yoon, J. H., *J. Photoscience* **2004,** 11, (1), 35-40.

(42) Powell, D. H.; NiDhubhghaill, O. M.; Pubanz, D.; Helm, L.; Lebedev, Y. S.; Schlaepfer, W.; Merbach, A. E., *J. Am. Chem. Soc.* **1996,** 118, (39), 9333-9346.

(43) Jaszberenyi, Z.; Moriggi, L.; Schmidt, P.; Weidensteiner, C.; Kneuer, R.; Merbach, A. E.; Helm, L.; Toth, E., *J. Biol. Inorg. Chem.* **2007,** 12, (3), 406-420.

(44) Crich, S. G.; Biancone, L.; Cantaluppi, V.; Esposito, D. D. G.; Russo, S.; Camussi, G.; Aime, S., *Magn. Reson. Med.* **2004,** 51, (5), 938-944.